Pergamon

Geochimica et Cosmochimica Acta, Vol. 67, No. 12, pp. 2239–2250, 2003
Copyright © 2003 Elsevier Science Ltd
Printed in the USA. All rights reserved
0016-7037/03 $30.00 + .00

doi:10.1016/S0016-7037(03)00023-1

Ubiquitous low-FeO relict grains in type II chondrules and limited overgrowths on phenocrysts following the final melting event

JOHN T. WASSON[1,2,3,*] and ALAN E. RUBIN[1]

[1]Institute of Geophysics and Planetary Physics
[2]Department of Earth and Space Sciences
[3]Department of Chemistry and Biochemistry, University of California, Los Angeles, CA 90095-1567, USA

(*Received June* 4, 2001; *accepted in revised form December* 18, 2002)

Abstract—Type II porphyritic chondrules commonly contain several large (>40 μm) olivine phenocrysts; furnace-based cooling rates based on the assumption that these phenocrysts grew in a single-stage melting-cooling event yield chondrule cooling-rate estimates of 0.01–1 K s^{-1}. Because other evidence indicates much higher cooling rates, we examined type II chondrules in the CO3.0 chondrites that have experienced only minimal parent-body alteration. We discovered three kinds of evidence indicating that only minor (4–10 μm) olivine growth occurred after the final melting event: (1) Nearly all (>90%) type II chondrules in CO3.0 chondrites contain low-FeO relict grains; overgrowths on these relicts are narrow, in the range of 2–12 μm. (2) Most type II chondrules contain some FeO-rich olivine grains with decurved surfaces and acute angles between faces indicating that the grains are fragments from an earlier generation of chondrules; the limited overgrowth thicknesses following the last melting event are too thin to disguise the shard-like nature of these grains. (3) Most type II chondrules contain many small (<20 μm) euhedral or subhedral phenocrysts with central compositions that are much more ferroan than the centers of the large phenocrysts; their small sizes document the small amount of growth that occurred after the final melting event. If overgrowth thicknesses were small (4–10 μm) after the final melting event, it follows that large fractions of coarse (>40 μm) high-FeO phenocrysts are relicts from earlier generations of chondrules, and that cooling rates after the last melting event were much more rapid than indicated by models based on a single melting event. These observations are thus inconsistent with the "classic" igneous model of formation of type II porphyritic chondrules by near-total melting of a precursor mix followed by olivine nucleation on a very limited number of nuclei (say, ≤10) and by growth to produce the large phenocrysts during a period of monotonic (and roughly linear) cooling. Our observations that recycled chondrule materials constitute a large component of the phenocrysts of type II chondrules also imply that this kind of chondrule formed relatively late during the chondrule-forming period. *Copyright © 2003 Elsevier Science Ltd*

1. INTRODUCTION

Porphyritic chondrules show two dominant textures: type I chondrules generally have many small (<20 μm) mafic silicate grains, whereas type II chondrules tend to have fewer and larger (>40 μm) grains (McSween, 1977; Scott and Taylor, 1983). In unequilibrated chondrites there is a strong relationship between textural type and composition; olivine fayalite values in the central areas of type I chondrules are commonly <5 mol.%, whereas fayalite values in type II chondrules are generally >10 mol.%. Many of the olivine phenocrysts in both types have compositional gradients that appear to be due to igneous zoning.

The commonly employed furnace method to determine cooling rates for type II chondrules yields rather low values in the range 0.01–1 K s^{-1} (Lofgren, 1996; Jones and Lofgren, 1993; Radomsky and Hewins, 1990). Low cooling rates are problematical because there is no plausible nebular environment that yields such values; cooling into cool (T < 1200 K) space yields cooling rates orders of magnitude higher, whereas cooling in a hot, opaque, nebular disk yields rates many orders of magnitude lower. For this reason, Wasson (1996) challenged the key assumption of the furnace-based simulations, i.e., that the texture was the result of a single heating/cooling event. He suggested that, at low ambient nebular temperatures, many chondrules experienced numerous small-scale flash-heating events that caused only minor degrees of melting; because the nebular temperature was <1000 K, each event was followed by rapid cooling. Rubin and Krot (1996) and Jones (1996) summarized evidence of relict grains, enveloping compound chondrules, and chondrule igneous rims that demonstrate that many chondrules experienced multiple melting events.

There is no doubt that the olivine in type II porphyritic chondrules grew largely from melt. In principle, coarse phenocrysts could have formed from melts with several nuclei that cooled very slowly or from homogeneous nucleation in nuclei-free melts that experienced a high degree of undercooling. However, dynamic crystallization experiments (Lofgren, 1989) indicate that the latter process produces barred textures rather than the typical porphyritic textures in which there are many mafic silicate grains having random orientations.

Yurimoto and Wasson (2002) modeled the O-isotopic and FeO/(FeO + MgO) gradients in a type II chondrule from the Yamato-81020 CO3.0 chondrite and inferred an extremely fast cooling rate at high temperatures. From the observed gradients in olivine composition and O isotopes in a relict assemblage in Y-81020 chondrule I, they inferred a cooling rate of ≈10^5 K s^{-1}. Although this high cooling rate is consistent with chondrule cooling in a cool nebula, the coarsest olivine phenocrysts (>200 μm) clearly could not have obtained their large dimen-

* Author to whom correspondence should be addressed (jtwasson@ucla.edu).

Table 1. Key properties of CO3.0 chondrules investigated in this study.

Chondrule[a]	Size[b] (μm)	Max. phenocryst size (μm)	Min. phenocryst Fa (mol%)	Max. phenocryst Fa (mol%)	Min. relict Fa (mol%)	Fragmental olivine present?
YcA	780 × 840	660	25.0	55.8	4.6	yes
YcI	480 × 620	380	26.2	71.8	15.4	yes
YcK	280 × 370	210	38.7	77.3	18.8	yes
YcL	220 × 280	130	21.8	40.8	16.4	yes
YcM	140 × 300	82	21.9	44.4	2.9	yes
AcD	220 × 370	230	29.6	n.d.	—	yes
AcE	140 × 160	82	24.2	51.9	17.8	yes
AcF	420 × 900	330	30.9	60.8	2.1	yes
AcG	52 × 83	37	36.9	38.5	12.6	yes
AcH	33 × 100	15	27.1	44.2	15.9	yes
AcI	150 × 160	85	30.7	37.9	18.3	yes

[a] "Y" chondrules are from Y-81020; "A" chondrules are from ALHA77307.
[b] Chondrule sizes are given as the maximum dimension and the maximum dimension perpendicular to this.
n.d. = not determined.

sions during monotonic cooling after the same melting event. Upon closer examination of this chondrule in the present study, we found that there were additional petrographic indications of rapid cooling; these include a cloud of small olivine grains that must have formed after the large phenocrysts had obtained dimensions close to those now present. Because of the primitive nature of CO3.0 chondrites, we focused our study on these least-altered carbonaceous chondrites.

2. SAMPLES AND ANALYTICAL METHODS

There are three known CO3.0 chondrites: Colony, Allan Hills A77307, and Yamato 81010. All are finds and weathered to different degrees. Our studies were carried out on sections of the two least weathered, Y-81020 and ALHA77307.

Back-scattered-electron (BSE) images were prepared using the UCLA Cameca CAMEBAX electron microprobe (EMP) and the UCLA LEO 1430 scanning electron microscope (SEM). EMP analyses of olivine and pyroxene grains were obtained with the Cameca CAMEBAX at UCLA. Analytical conditions were a 15-kV accelerating potential, 10–20 nA beam currents, 20-s counting times, and a focused beam. Natural and synthetic mineral standards and Pouchou and Pichoir corrections (the Cameca version of ZAF corrections) were employed.

3. OBSERVATIONS

We examined 11 type II chondrules and chondrule fragments; five in section Y-81020,56-4 and six in section ALHA77307,88. Each chondrule was designated by a letter; in one case the same letter was used for both chondrites. We use shorthand abbreviations for each chondrule in which the first letter refers to the chondrite name and the last letter to the specific chondrule. For example, YcI stands for Y-81020 chondrule I and AcE stands for ALHA77307 chondrule E.

Basic information about the chondrules is summarized in Table 1. BSE images of some chondrules are shown in Figures 1 and 2. All chondrules in this study have type II textures consisting of relatively large olivine phenocrysts (as well as smaller ones) embedded in a feldspathic mesostasis. Most mesostases contain crystallites of Ca-pyroxene and accessory to minor amounts of opaque phases (metallic Fe-Ni, troilite, and chromite). Olivine phenocrysts are FeO-rich and appear relatively bright in BSE images. Present along with the olivine phenocrysts in every chondrule we studied are angular anhedral FeO-rich olivine grains that appear to be phenocryst fragments.

Low-FeO olivine relicts inside some FeO-rich olivine phenocrysts show up as dark patches near the centers. Although there are compositional discontinuities between the low-FeO relict grains and the surrounding high-FeO olivine, in many cases there is a halo of intermediate-composition olivine around the relict grain. This halo of intermediate darkness in the BSE images may be indicative of mixing between the relict grain and the surrounding matter, perhaps by solid-state diffusion, perhaps reflecting the presence of a boundary layer melt. Alternatively, in some cases the halo could be a second-generation relict grain, i.e., an overgrowth on the original relict grain formed during a previous episode of low-degree melting of the chondrule.

We tabulate in Table 1 the fayalite values measured near the centers of large olivine phenocrysts; these range from Fa22 to Fa39. Phenocryst rim compositions in these chondrules are always more FeO-rich, ranging in composition from Fa38 to Fa77 (Table 1).

We first describe the properties of chondrules in Y-81020 (Figs. 1 and 2), then those in ALHA77307 (Fig. 3). We made the most extensive observations on YcI and therefore describe it first. Thereafter, we describe the chondrules in alphabetical order.

YcI is a relatively large (480 × 620 μm) type II (FeO-rich) porphyritic olivine chondrule (Fig. 1a). It contains three coarse olivine phenocrysts. We follow the nomenclature of Yurimoto and Wasson (2002) and number the grains in order of decreasing size: the largest grain is grain 1 (subhedral), 240 × 380 μm; the next largest is grain 2 (anhedral and fragmented), 170 × 200 μm; grain 3 (subhedral) is 120 × 210 μm. The fourth largest olivine phenocryst is perhaps better described as a crystal clot; it is 81 × 93 μm and contains a relict grain, described below (Fig. 1b) and in more detail by Yurimoto and Wasson (2002). Plucking during thin section preparation resulted in the formation of a large (120 × 180 μm) hole in the center of the chondrule. Feldspathic mesostasis containing small (1–4 × 2–90 μm) elongated Ca-pyx crystallites (Fig. 1a,b) constitutes ~18 vol.% of the chondrule (if we make the assumption that mesostasis constituted 80 vol.% of the large hole). Alongside portions of phenocryst grains 2 and 3 are small (2–14-μm-size) intergrown, euhedral-to-subhedral olivine grains that resemble a cluster of cauliflower florets (Fig.

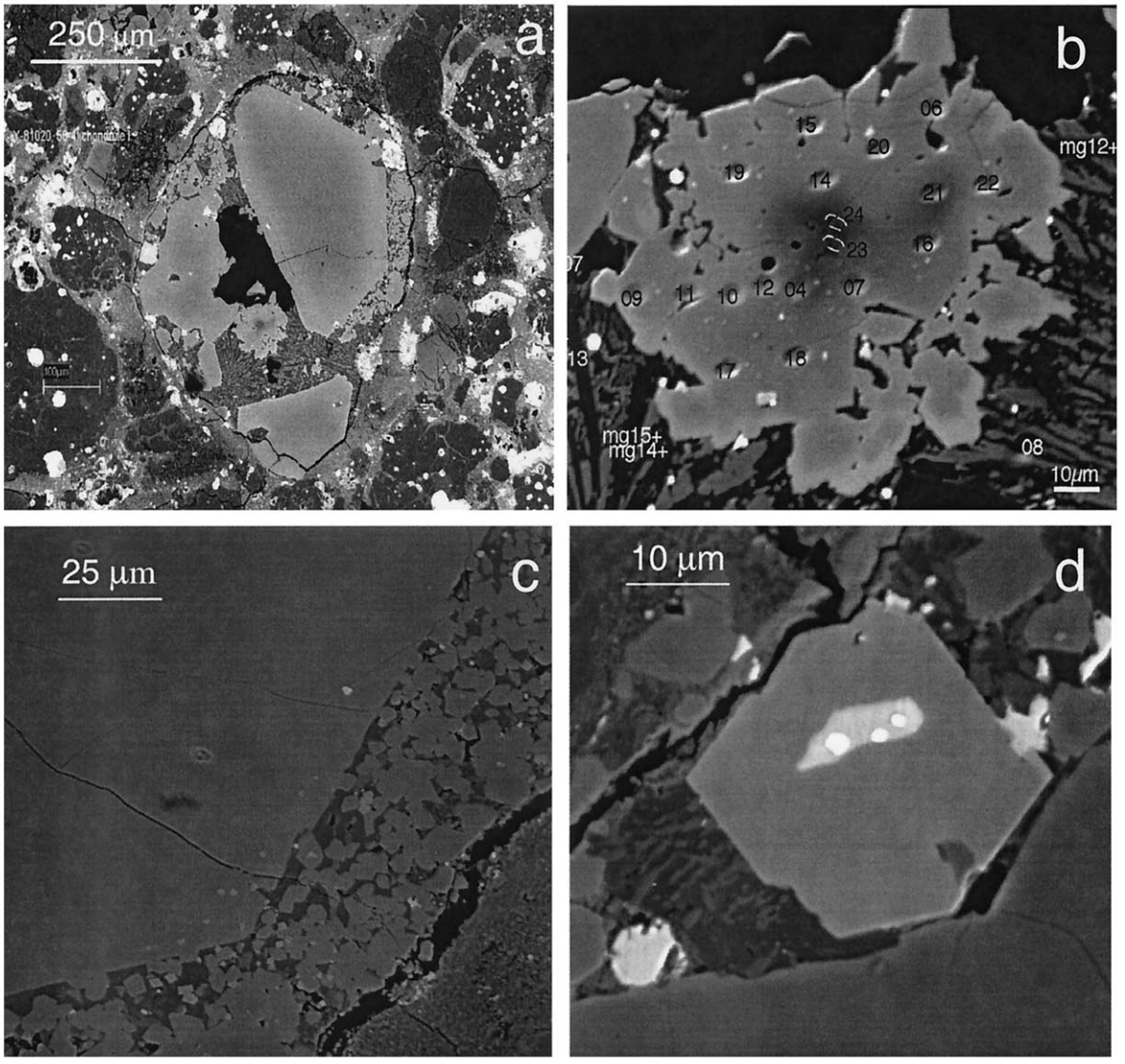

Fig. 1. Chondrule YcI. (a) Entire chondrule showing coarse ferroan olivine phenocrysts (light gray), feldspathic mesostasis (dark gray), and included Ca-pyroxene crystallites (intermediate gray). A large dark hole (black) due to plucking during thin section preparation occurs in the middle of the chondrule. Large grain at top center, above and to the right of the hole is grain 1. Just beneath the hole is grain 4 which contains a relict grain (dark patch in center). (b) Olivine phenocryst 4 containing the low-FeO relict grain (dark patch). Elliptical shapes in the phenocryst are ion-probe pits. The numbers in the pits are keyed to O- and Mg-isotopic analyses of Yurimoto and Wasson (2002). Phenocryst 4 is partly surrounded by feldspathic mesostasis (dark gray) containing Ca-pyroxene crystallites (intermediate gray). (c) Portion of grain 1 showing small chromite grains (very light gray) near the periphery of the phenocryst and subparallel to the grain boundary. Small intergrown FeO-rich "cauliflower" olivine grains (light gray) and associated chromite (very light gray) in the mesostasis (dark gray) outside grain 1 formed after the final melting event. (d) Coarse euhedral chromite grain nestled between olivine phenocryst 2 (the coarse grain at the left margin of the chondrule in Fig. 1a) and the chondrule boundary. The chromite grain contains an elongated patch of troilite (light gray) with three round blebs of tetrataenite (white) inside. All images by back-scattered electrons (BSE).

1c). Also present in the mesostasis (and adjacent to some of the small olivine grains) are 2–10-μm-size euhedral chromite grains (Fig. 1c). Some intermediate-size ($\sim$40 μm) olivine grains contain chromite grains inside them. About two dozen 1–2-μm-size euhedral chromite grains are present within phenocryst 1 (Fig. 1c); the chromite grains occur 4–15 μm from the edge of the grain subparallel to the grain boundary along $\sim$40% of the grain's perimeter. Adjacent to grain 2 is a relatively large (27-μm) euhedral chromite grain (Fig. 1d) containing an elongated 4 $\times$ 12-μm-size patch of troilite that includes three small (1.0–1.5-μm-size) blebs of tetrataenite.

Grain 4 (Fig. 1b) contains a few dark patches in BSE images indicative of relict grains. The dark patch with the lowest FeO is Fa15.4. Grain 4 also contains a $\sim$20-μm-size patch that has an Al-rich bulk composition (in wt.%): SiO_2, 42.2; Al_2O_3, 22.0; MgO, 16.4; FeO, 7.3; MnO, 0.14; CaO, 11.4; Na_2O, 0.12).

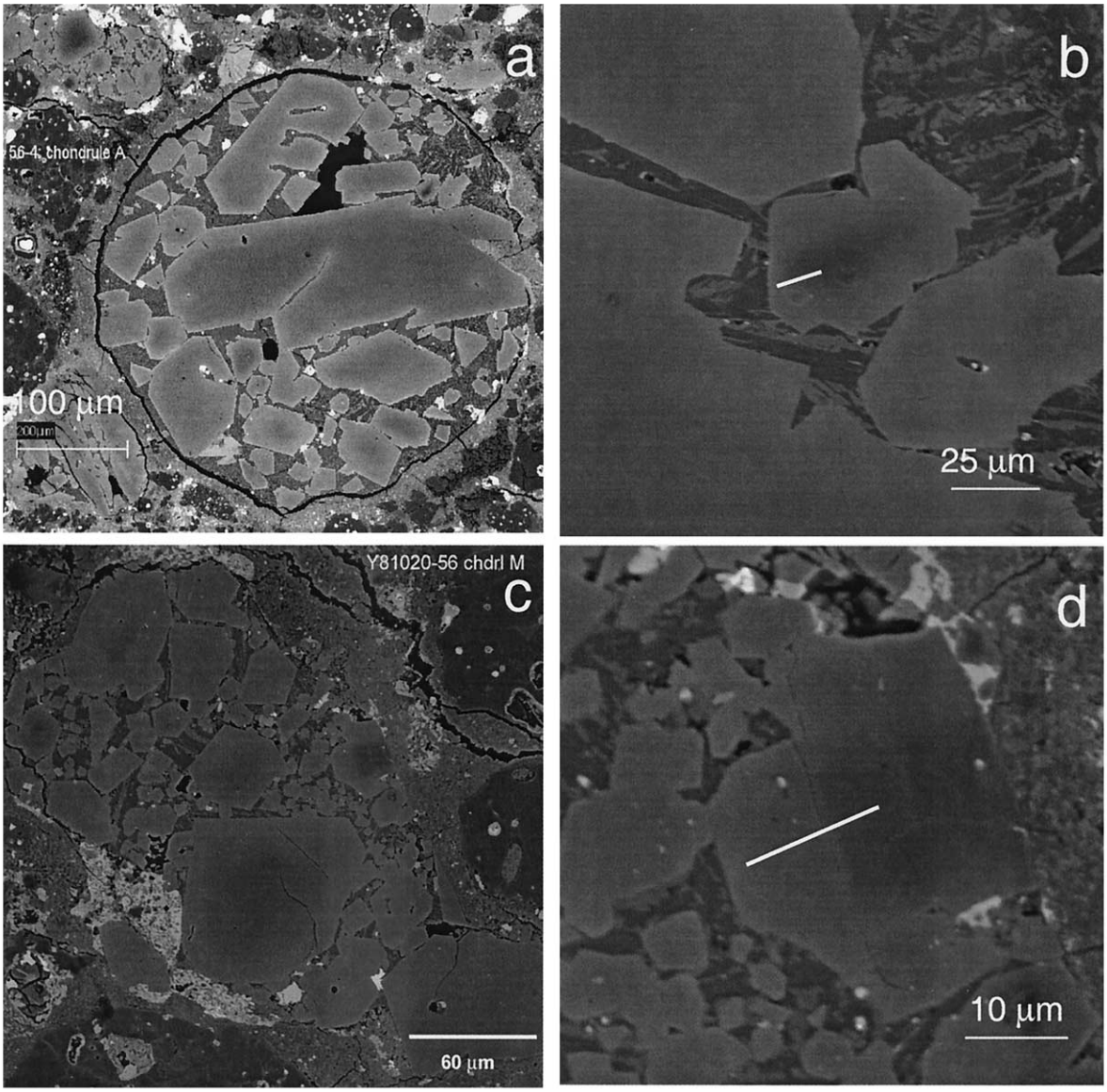

Fig. 2. Type II porphyritic olivine chondrules and relict grains in the Y-81020 CO3.0 chondrite. (a) Chondrule YcA contains a coarse ferroan olivine phenocryst (grain 1, center), a skeletal olivine grain (grain 2, top), and several other subhedral and anhedral phenocrysts. (b) The relict grain (dark gray patch) in YcA occurs in the center of a small ferroan olivine grain (grain 8) that is located just above grain 1 (in Fig. 2a) to the right of center. The white line in the grain is the trace of the zoning profile illustrated in Figure 4a. Grain 8 is flanked by two other ferroan olivine phenocrysts and is partly surrounded by feldspathic mesostasis (dark gray) containing Ca-pyroxene crystallites (intermediate gray). (c) Chondrule YcM with its coarse ferroan olivine phenocrysts with dark centers and light-shaded rims. A phenocryst with a relict low-FeO olivine grain occurs at the right center of the chondrule. (d) A phenocryst fragment containing a rectangular relict grain in YcM located near the present boundary of the fractured chondrule. The white line in the grain is the trace of the zoning profile illustrated in Figure 4b. All images by BSE.

Yurimoto and Wasson (2002) suggested that the patch formed as melt when an amoeboid-olivine-inclusion-like precursor of the current assemblage was incompletely melted.

The coarse olivine phenocrysts exhibit normal igneous zoning ranging from Fa26 in grain centers to Fa57 within 1 μm of the grain edge. The small cauliflower grains, which appear to have crystallized after the final melting event, have compositions of Fa45–65. Rare olivine grains surrounded by mesostasis are even more ferroan, ranging up to Fa72.

YcA (Fig. 2a) is the largest chondrule in the Y-81020 section (780 $\times$ 840 μm). It contains one very large (230 $\times$ 660 μm) subhedral phenocryst and ~60 additional phenocrysts in the plane of the section ranging from 15 to 330 μm in maximum dimension. The second largest phenocryst (150 $\times$ 330 μm) has a moderately skeletal morphology. Feldspathic mesostasis containing small (typically 1 $\times$ 25 μm) elongated Ca-pyroxene crystallites constitutes ~20 vol.% of the chondrule. Five low-FeO relict olivine grains (with compositions as magnesian as

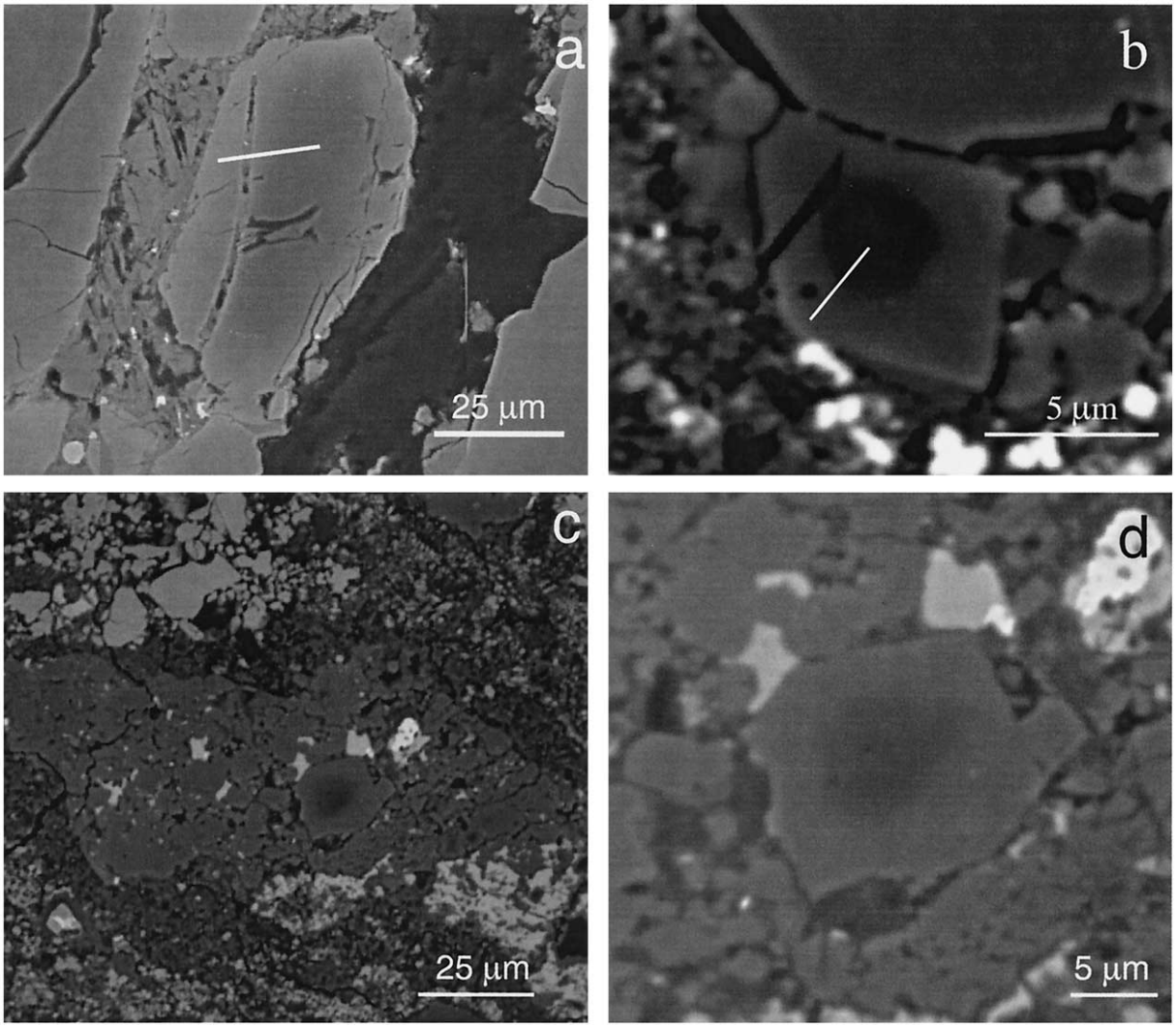

Fig. 3. Type II porphyritic olivine chondrules and relict grains in the ALHA77307 CO3.0 chondrite. (a) Relict grain (dark gray patch) in chondrule AcF occurs in the middle of an elongated ferroan olivine grain fragment (grain 3). The white line in the grain is the trace of the zoning profile illustrated in Figure 4c. (b) Small relict grain (dark gray patch) surrounded by a ferroan olivine overgrowth (grain 1) in chondrule AcG. The white line in the grain is the trace of the zoning profile illustrated in Figure 4d. (c) Chondrule fragment AcH consists largely of small ferroan olivine phenocrysts (many of which are angular fragments). The mesostasis content is very low. A phenocryst containing a relict low-FeO olivine occurs in the chondrule center. (d) Subhedral ferroan olivine phenocryst in AcH containing a rounded low-FeO olivine relict grain. All images by BSE.

Fa4.6) surrounded by ferroan olivine phenocrysts are present in the plane of the section (e.g., grain 8; Fig. 2b). A compositional zoning profile across the low-FeO relict and overgrowth in grain 8 (Fig. 4a) is very steep, showing little elemental exchange between the relict and the overgrowth. The large olivine phenocrysts exhibit igneous zoning with a maximum range in an individual grain of Fa25 in the center to Fa56 at the margin.

YcK (Fig. 5) is a fragment, but its radius of curvature indicates that ~80% of the chondrule is present. It contains one very coarse, quasi-equant olivine grain (grain 1, 180 × 210 μm) and an elongated, segmented, moderately skeletal grain (grain 2, 80 × 350 μm) that curves around the inside margin of the chondrule. Mesostasis constitutes ~10 vol.% of YcK. It appears plausible that grain 1 contains two generations of relict grains. In the center there is a 65-μm-size (dark gray) relict, representing the earliest generation of olivine. This grain appears somewhat angular and has a minimum fayalite composition of Fa18.8. The relict is surrounded by a 110-μm-wide (intermediate gray) patch that we interpret as a second-generation relict that overgrew the first relict before the final melting event. This olivine has a minimum composition of Fa39. The right side of this second-generation grain can be traced within 10 μm of the mesostasis, thus providing an estimate of the overgrowth thickness in the final melting event; the apparent ~50 μm thickness of the overgrowth in the left and bottom side of the grain is an overestimate due to geometric effects. This second-generation grain is in turn overgrown by ferroan olivine similar in composition to the large, segmented grain (grain 2). In grain 1, dozens of micrometer-size opaque grains (chromite and sulfide) occur near the outer margin of (and surround) the

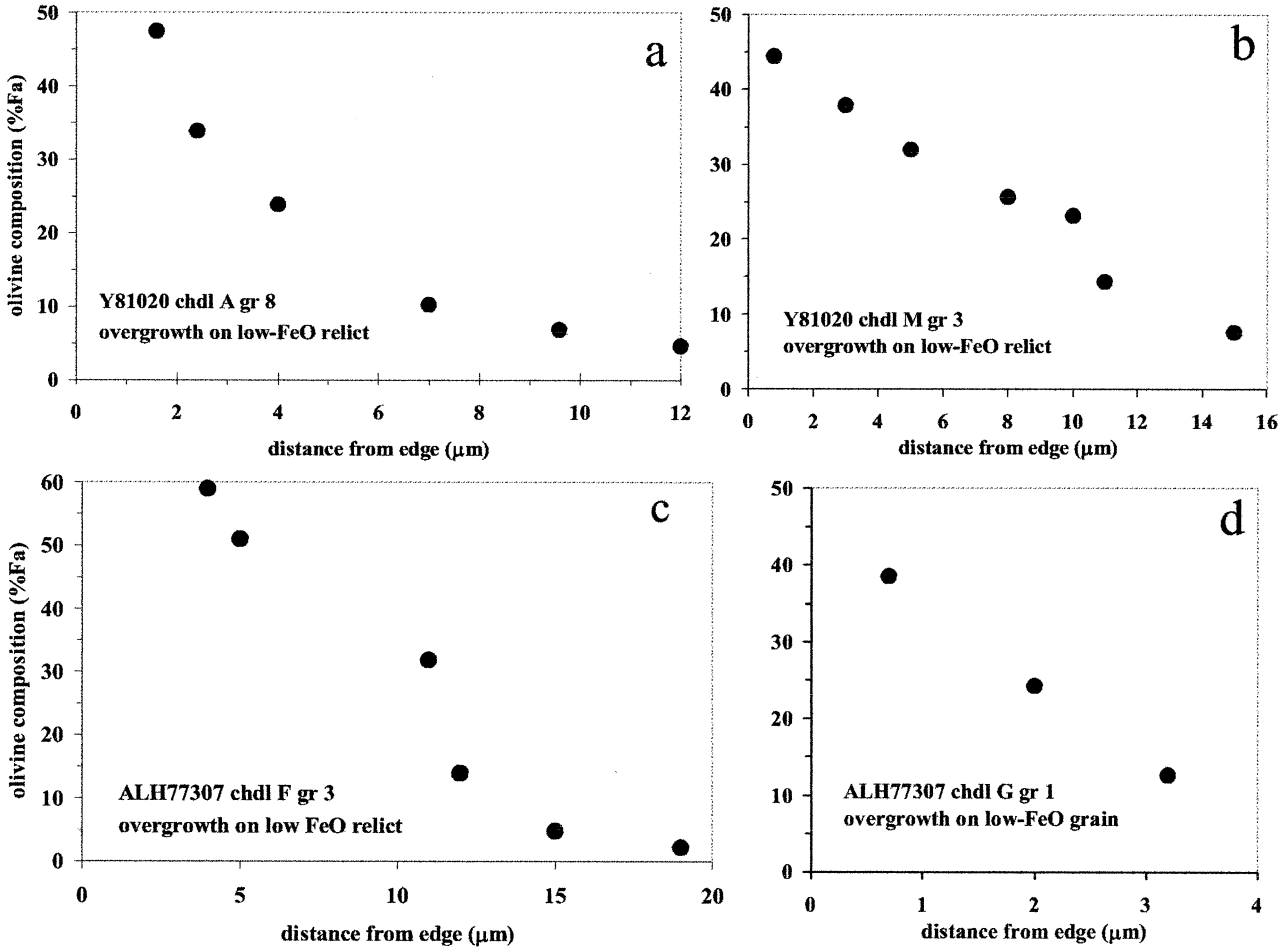

Fig. 4. Compositional zoning profiles demonstrate that the high-FeO olivine overgrowths on low-FeO relict olivine grains are quite narrow. The slightly elevated regions near the low-FeO substrates are attributed to crystallization of a boundary liquid produced largely by minor melting of the relict. Minor degrees of scatter are probably due to uncontrolled geometric effects. (a) Grain 8 in chondrule YcA. (b) Grain 3 in chondrule YcM. (c) Grain 3 in chondrule AcF; the small elevation of the point at 10 μm may represent electron beam overlap of a crack or EMP fluorescence of neighboring FeO-rich materials. (d) Grain 1 in chondrule AcG grain 1. Overgrowth thicknesses on the relict olivine grains range from 2 to 12 μm.

second-generation "relict" overgrowth. The highest fayalite composition reached at the periphery of grain 1 (within 2 μm of the edge of the grain) is Fa77. We cannot completely discount the alternative view of grain 1; i.e., it could contain a single low-FeO relict grain that underwent extensive diffusion with the FeO-rich overgrowth. However, this scenario does not account for the apparently sharp boundaries between the dark gray and intermediate gray regions. It is also uncertain when diffusion occurred: Y-81020 is among the least-metamorphosed chondrites. In addition, we infer that the chondrule cooled quickly, leaving little time for auto-metamorphism. We thus conclude that grain 1 most likely represents two generations of relict grains.

YcL (Fig. 6d) consists of one large (90 $\times$ 130 μm) subhedral olivine phenocryst (grain 1) and ~10 others (in the plane of the section) ranging from one-quarter to one-half the size of grain 1. Some of these grains are euhedral; a few are angular fragments. Feldspathic mesostasis containing numerous tiny (typically ~1 $\times$ 6 μm) Ca-pyroxene crystallites constitutes ~20 vol.% of the chondrule. One 50 $\times$ 65 μm olivine phenocryst (bottom right of Fig. 6d) contains an 8-μm-diameter low-FeO (Fa16.4) relict olivine grain. The large olivine phenocrysts exhibit normal igneous zoning with a maximum range of Fa22 to Fa41. The BSE image shows that the FeO/(FeO + MgO) gradient is high at the border of the relict; if this low-FeO olivine core had grown in situ (i.e., was formed in equilibrium with the bulk melt), the gradient would be small to negligible.

YcM is an elongated chondrule, 140 $\times$ 300 μm in size (Fig. 2c). It contains euhedral, subhedral, and anhedral olivine phenocrysts in a large range of sizes from a quasi-equant subhedral grain (grain 1, 90 $\times$ 100 μm) down to 2-μm-size intergrown grains. Ca-pyroxene crystallites in the matrix range from 3 to 25 μm in length. The mesostasis constitutes ~6 vol.% of YcM. Two low-FeO relict olivine grains are evident, a 16-μm-size rounded relict (Fa5.8) in grain 1 and a 17-μm-size rectangular relict (Fa2.9) in grain 3 (Fig. 2d). The latter grain exhibits a linear compositional zoning profile (Fig. 4b). The large olivine phenocrysts are normally zoned, ranging from Fa22 to Fa44.

AcD is the only chondrule in this study that does not have a relict grain apparent in the plane of the section. The chondrule

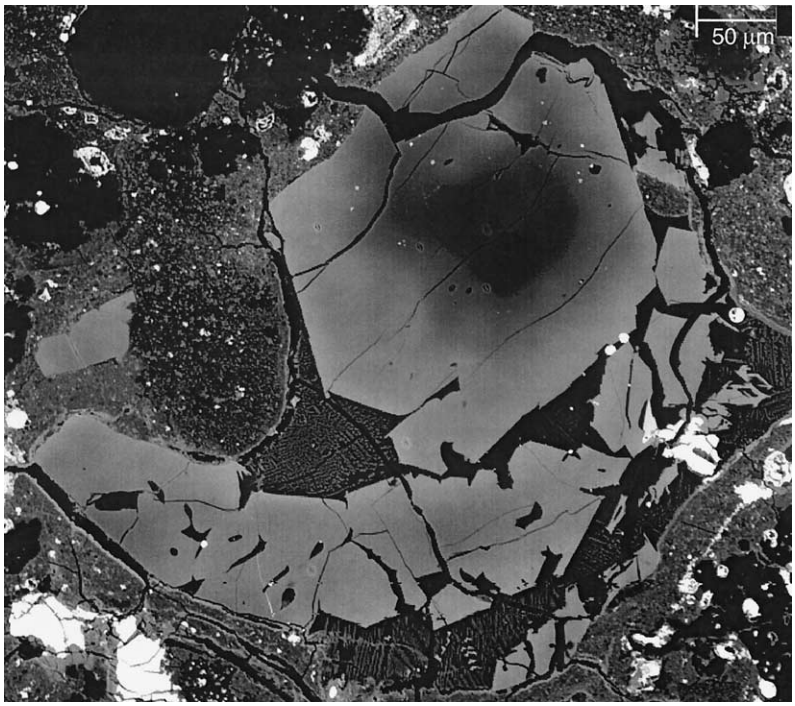

Fig. 5. Chondrule fragment YcK which contains a coarse, quasi-equant olivine phenocryst (grain 1) and an elongated segmented olivine crystal (grain 2). Grain 1 appears to contain two generations of relict grains. At the center of grain 1, an angular dark low-FeO patch represents the earliest relict. This is surrounded by a larger, lighter-gray patch that is also somewhat angular; this patch is the second-generation relict grain. The latter grain is overgrown by ferroan olivine similar in composition to the olivine in grain 2. A BSE image.

consists of one large subhedral phenocryst (grain 2, 190 × 230 μm) and several smaller subhedral and anhedral olivine grains. The center of the second largest grain (grain 1, 90 × 100 μm) has olivine of Fa29.6. Mesostasis containing small crystallites of Ca pyroxene constitutes only a small fraction of AcD (<3 vol.%).

AcE contains coarse subhedral, anhedral, and angular olivine phenocrysts ranging from 13 to 82 μm in maximum dimension. Mesostasis with Ca-pyroxene crystallites constitutes 2–5 vol.% of the chondrule. Two low-FeO relict olivine grains are evident in the chondrule. A 5-μm-size relict (Fa17.8) occurs in grain 3 (25 × 35 μm), and a 2-μm-size relict (Fa18.0) occurs in grain 1 (a 15 μm-size equant grain). The ferroan olivine phenocrysts exhibit normal igneous zoning with a maximum range of Fa24 to Fa52.

AcF is a large elongated chondrule fragment (420 × 900 μm); there are no curved surfaces and it is impossible to determine the original size of the chondrule. The chondrule contains coarse (up to 150 × 330 μm) and intermediate-size (typically 60–125 μm) olivine phenocrysts, relatively coarse (typically 5 × 15 μm) interstitial Ca pyroxene, and little feldspathic mesostasis. There are two low-FeO relict olivine grains visible in the plane of the section. The 25 × 40 μm relict in subhedral ferroan olivine grain 1 (60 × 70 μm) has a composition of Fa4.0; the 13 × 18 μm relict in elongated ferroan olivine grain 3 (35 × 70 μm) (Fig. 3a) has a composition of Fa2.1. The latter grain exhibits a very steep compositional gradient (Fig. 4c), consistent with little elemental exchange between the low-FeO relict and the high-FeO overgrowth. The large olivine phenocrysts are normally zoned, exhibiting a maximum compositional range of Fa31 to Fa61.

AcG contains ferroan olivine grains ranging in size from 1.5 μm to 32 × 37 μm. All of the largest grains and many smaller ones are anhedral and fragmental; the chondrule appears to have been crushed. The only relict low-FeO olivine grain in the plane of the section (2 × 3 μm; Fa12.6) occurs in a small euhedral, diamond-shaped ferroan olivine (grain 1, 7 × 9 μm) (Fig. 3b). The small size of its overgrowth rim (~2 μm) may reflect paucity of mesostasis (<2 vol.% is present in the chondrule). The grain exhibits linear compositional zoning (Fig. 4d). The large olivine phenocrysts are normally zoned, but the gradients are very shallow; compositions range only from Fa37 to Fa38.

AcH is a small, elongated chondrule fragment (33 × 100 μm); the lack of curved surfaces makes it impossible to determine the original size of the parent chondrule (Fig. 3c). The chondrule fragment contains small euhedral, subhedral, and anhedral (fragmental) ferroan olivine grains ranging only up to 13 × 15 μm for the largest grain (grain 1). Grain 1 also contains the only relict low-FeO olivine grain in AcH; the relict is a rounded, 4.4-μm-diameter object (Fig. 3d) of composition Fa15.9 that is surrounded by a steep gradient. AcH contains ~3 vol.% mesostasis containing small grains of Ca pyroxene. The ferroan olivine phenocrysts are normally zoned, ranging in composition from Fa27 to Fa44.

AcI is a nearly equant object (150 × 160 μm) containing a few coarse subhedral olivine phenocrysts (typically 35–65 μm) and fragmental olivine grains as small as 5 μm. The chondrule

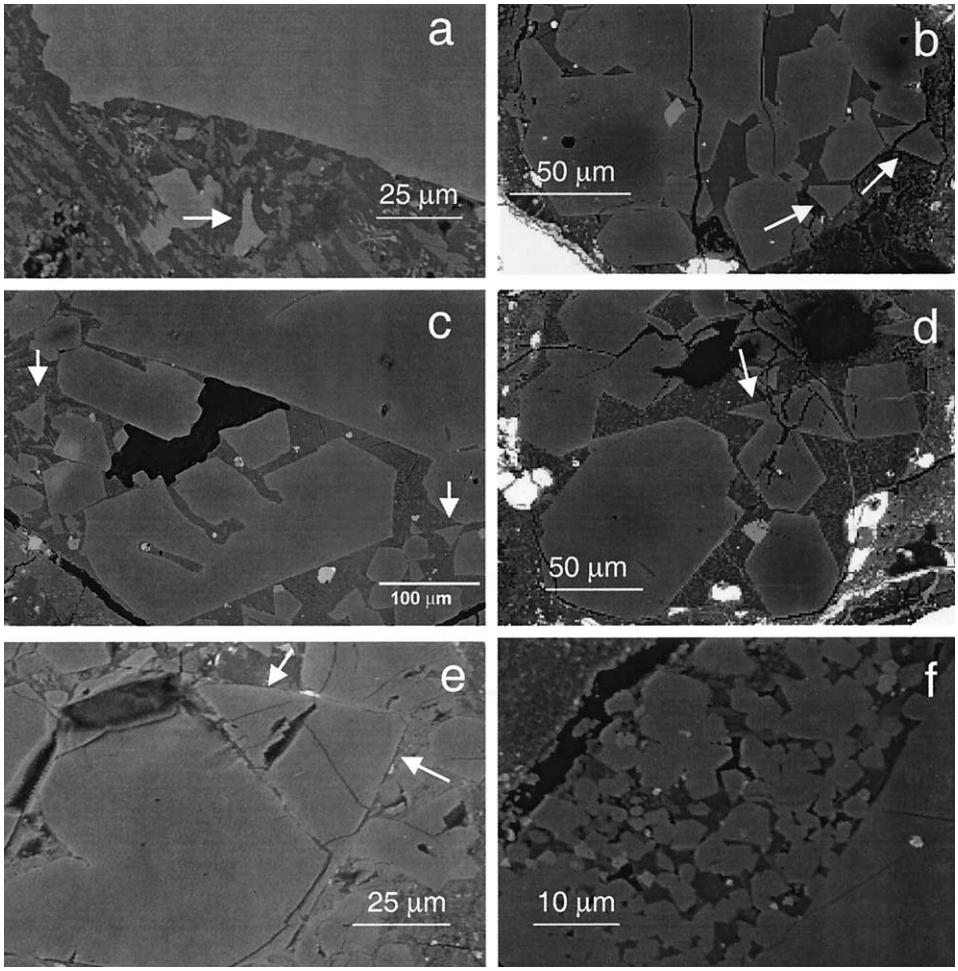

Fig. 6. Shards and crystals in type II chondrules in Y-81020. (a) Portion of YcI showing a scalloped ferroan olivine grain fragment (arrow) surrounded by mesostasis (bottom center). (b) Portion of YcN containing quasi-triangular ferroan olivine fragments (arrows; right side). (No compositional information was obtained for this chondrule, so it is not listed in Table 1 or 2). (c) Portion of YcA showing quasi-triangular ferroan olivine grain fragments (arrows; left center and right center). (d) Portion of YcL showing a large triangular ferroan olivine grain fragment (arrow; right of center) impinging on a subhedral ferroan olivine grain. (e) Triangular olivine grain (arrows) in a portion of chondrule AcE. (f) Small cauliflower olivines (intermediate gray) and chromite grains (light gray) in the mesostasis adjacent to coarse grain 1 (bottom right). These small grains crystallized from the melt following the final melting event. The cauliflower grains (also shown in Fig. 1c) have the typical shapes of olivine grains that grow from small nuclei. All images by BSE.

contains 5–8 vol.% feldspathic mesostasis containing small grains of Ca pyroxene. One olivine grain (grain 3) (32 × 36 μm) contains a small (~7 μm), rounded low-FeO olivine relict (Fa18.3). The other olivine phenocrysts are normally zoned, but exhibit shallow compositional gradients, e.g., Fa31 to Fa38.

In addition to these well-studied chondrules, we made SEM images of 30 other type II chondrules and chondrule fragments in section Y-81020,56–4. They all contain coarse ferroan olivine phenocrysts, smaller olivine grains of similar composition, and feldspathic mesostasis. Twenty-eight of the objects contain evident low-FeO relict olivine grains with ferroan olivine overgrowths. One object (W8) contains eight relict grains in the plane of the section. About 20% of the chondrules have rings of small opaque grains (mostly chromite) within (but near the outer boundaries of) the relicts or just outside them at the border between the relicts and the ferroan olivine overgrowths.

4. DISCUSSION

4.1. Detailed Study of Y81020 Chondrule

We began our study with Yamato 81020 chondrule I (Fig. 1) because Yurimoto and Wasson (2002) inferred that very fast (ca. 10^5 K s^{-1}) cooling rates were necessary to explain the observed gradients in olivine composition and O isotopes in a relict assemblage. Such high rates are consistent with the chondrule having cooled by radiation into cool space (Hood and Kring, 1996; Wasson, 1996). Although this cooling rate applies at temperatures >100 K higher than those at which most olivine crystallized, this temperature difference is not enough to reconcile this rate with those inferred from furnace simulations of type II structures (the highest of which are ~1 K s^{-1}). Thus, the key question we are addressing is whether this relict assemblage and the large olivine phenocrysts in this chondrule

Table 2. Summary of relict grain properties in the CO3.0 chondrules investigated in this study.

Chondrule[a]	Max. relict size (μm)	Min. relict Fa (mol%)	Apparent overgrowth (μm)
YcA	18	4.6	7
YcI	20	15.4	22
YcK[b]	110	18.8	9
YcL	8	16.4	8
YcM	17	2.9	9
AcD	none	—	—
AcE	5	17.8	2
AcF	40	2.1	12
AcG	3	12.6	2
AcH	6	15.9	2
AcI	5	18.3	4

[a] "Y" chondrules are from Y-81020; "A" chondrules are from ALHA77307.

[b] YcK exhibits two generations of relict crystals: the earliest crystal is 65 μm in size; the second-generation crystal is 110 μm. The 9-μm overgrowth formed during the final melting event and is on the second-generation relict grain.

formed in the melting event modeled by Yurimoto and Wasson, or whether much of their growth occurred in earlier melting events. If the latter seems more probable, it is then important to compare the evidence in YcI with observations on other type II chondrules in CO3.0 chondrites.

The minimum FeO/(FeO + MgO) ratio in grain 1 (the largest phenocryst) in YcI is ~0.26. Minimum fayalite values taken in the centers of the other two large phenocrysts are still greater. A rough estimate of the initial FeO/(FeO + MgO) ratio in the melt that produced grain 1 is 0.50. From this value, it is clear that the lowest fayalite content observed in phenocryst 4 (Fa15.4; Table 2) is far out of equilibrium.

Because this phenocryst (Fig. 1b) seems to consist of numerous small grains fused together (a "crystal clot") and has an irregular shape, it is not readily compared with the grains discussed below. Thus, the "overgrowth thickness" listed in Table 2 was not formed by plane-front growth but by three-dimensional formation and growth on many relict nuclei.

The structure of chondrule YcI seems to require that there were numerous (possibly hundreds or thousands) nuclei present at the time of the final melting event experienced by this chondrule. This is counter to the interpretation that large phenocrysts are formed because there were only a few nuclei available (Jones, 1990; Lofgren, 1996). It is clear that each of the cauliflower phenocrysts (Figs. 1c, 6f) grew on a preexisting nucleus following the final melting event.

If these grains were growing from a well-mixed, near-total melt (i.e., one that encompassed most of the chondrule) in competition with phenocryst 1, they should have grown at the same rate. Within this scenario, it is difficult to understand how grain 1 could have grown to dimensions of ≥480 μm while other grains were growing only to sizes of 2–14 μm. We can reject the possibility that impingement limited the growth of the small grains because those grains that are adjacent to mesostasis are no larger than the remainder. In some cases, patches of mesostasis 10–20 μm across have small cauliflower grains on one side and grain 1 on the other.

Experimental synthesis of chondrules offers support for our interpretation. Olivine phenocrysts grown during crystallization experiments (at modest cooling rates and moderate degrees of undercooling) tend to have euhedral or euhedral/skeletal morphologies with characteristic interfacial angles (Donaldson, 1976; Hewins, 1988). Crystals grown at very rapid cooling rates and at substantial degrees of undercooling develop barred or feathery morphologies (Fig. 8 of Donaldson, 1976; Figs. 5 and 7 of Tsuchiyama et al., 1980). If substantial numbers of nuclei are present in the charge during a flash-heating experiment, then relatively narrow overgrowths of ferroan olivine form on the preexisting crystals (Fig. 3 of Connolly and Hewins, 1996). There does not appear to be a realistic way of forming the cauliflower grains than by growing them from a cloud of nuclei present in the melt.

The acute angles formed at some olivine grain edges in the type II chondrules (Fig. 6a–e) do not match the interfacial angles of olivine grains grown during crystallization experiments (e.g., Fig. 9. 2.2c of Hewins, 1988); they are thus likely to be grain fragments. There is another problem with the near-total melt model. All of the olivine grains in an individual chondrule such as YcI should have begun to grow with the same initial composition, roughly the value of Fa26 that we measured in the center of grain 1. However, the lowest Fa content observed in the center of the cauliflower grains in this chondrule is 47 mol.%, a value that would only be reached after extensive (>50%) crystallization of an original, near-total melt had occurred. Such a high Fa value is similar to that of the outer 10-μm portion of grain 1. It seems quite clear from these arguments that only a minor, FeO-rich portion of the chondrule was melted during the last melting event experienced by chondrule YcI.

There are abundant chromite grains in the cauliflower region (Fig. 6f), and an interesting set of roughly aligned small chromite grains located 8–10 μm from the adjacent surface of grain 1 (Fig. 1c). We suggest that, after the final, minor melting event, this area of mesostasis was Cr-rich (e.g., this part of the precursor happened to contain some crushed chromite probably produced together with the olivine nuclei of the cauliflower grains). After a small amount of olivine crystallization occurred, chromite became a liquidus phase, and some chromite nucleated in the overgrowth portion of grain 1. During continuing crystallization, no new chromite nuclei formed; the Cr content of the melt became relatively low and much of the remaining Cr was able to diffuse to small chromite grains in contact with the melt. The coarse euhedral chromite grain on the other side of YcI (Fig. 1d) is probably relict (i.e., it was not formed during the final melting event); its presence signifies that the chondrule precursor had substantial Cr. We infer that this chromite grain is a relict on the basis of its large size; it is more than 300 times larger in cross-sectional area than typical chromite grains in the chondrule mesostasis.

These interpretations allow us to estimate that the maximum amount of overgrowth on grain 1 was 8–10 μm. Geometrical corrections would be needed if this part of grain 1 is not sectioned perpendicular to the surface; in that case, the maximum overgrowth would be even less.

4.2. Evidence in Other Chondrules Regarding Their Cooling Histories

Our survey of CO3 type II chondrules revealed that many show evidence that the layer of new olivine grown after the last melting event was relatively thin, and thus that the cooling rate

after this event was relatively rapid. There are three kinds of evidence that support this conclusion: (1) thin ferroan olivine overgrowths; (2) clusters of many small FeO-rich grains (e.g., cauliflower grains) in the mesostasis; and (3) small, angular fragmental olivine grains.

Perhaps the most compelling evidence is the fact that thin overgrowth layers are found on all the relict grains that are present in nearly every type II chondrule. This overgrowth is clearly visible for one relict grain in YcA (Fig. 2b). The olivine profile measured in this grain plotted in Figure 4a shows that the thickness of the overgrowth is ~8 μm.

With the exception of the overgrowth on the crystal clot (as noted above, not a single grain) in YcI (Fig. 1b), these overgrowths are in the range 2–12 μm (Table 2). If we neglect the (possibly impinged) 2-μm overgrowth on the small relict grain in AcG, the mean overgrowth thickness is 6 μm. Because in most cases the overgrowth was not sectioned perpendicular to the grain–mesostasis interface, the values obtained by us are upper limits on the true thicknesses of the overgrowths. We will therefore use 4 μm as a working mean value of overgrowth thickness.

Judging from the relative uniformity in overgrowth thickness, we infer that all these type II chondrules experienced similar cooling histories. After the final melting event, they were only able to grow layers of approximately 4 μm in thickness (within a factor of 2 or so). This seems to imply cooling rates orders of magnitude faster than the highest values (ca. 1 K s^{-1}) inferred from furnace-based simulations of type II structures (Lofgren, 1996).

The traditional model to form the very coarse grains common in type II chondrules is as follows: (1) a near-total melt forms; (2) only a handful of nuclei survive in the melt; and (3) the melt cools slowly enough to allow each grain to feed on a large volume of mesostasis, thus growing to a large size. There are three related kinds of evidence in our set of CO chondrules that are inconsistent with this model. (a) In most type II chondrules there are many small grains that did not grow to large dimensions despite being in contact with the mesostasis; (b) the centers of these small grains are too ferroan to have grown from the initial melt (i.e., the one that produced the large phenocrysts with appreciably lower FeO in their centers); and (c) there are other olivine grains in the mesostasis that exhibit shapes that are fragmental (i.e., angular rather than euhedral), an indication that the layer of overgrowth was too thin to disguise the fragmental nature of these grains. In each type II chondrule, we observed small (10–40 μm), angular fragments (Figs. 2a, 6a–e) that we interpret as crushed phenocrysts from earlier chondrule generations.

In YcI we observed an abundance of tiny FeO-rich olivine grains that we call cauliflower. Compositions of the centers of these grains are Fa ≥ 47, a clear demonstration that these grains did not nucleate at the same time as the adjacent large grain 1 that has Fa26 olivine in its center. Although some of these small grains stopped growing because they impinged on each other, this seems to have been a minor effect because other grains adjacent to mesostasis are not appreciably larger.

4.3. Does the Olivine Growth Rate Depend on the FeO/(FeO + MgO) Ratio in the Substrate Olivine?

G. Lofgren (private communication, 2002) noted that the size of the olivine unit cell increases as the FeO/(FeO + MgO) ratio increases, and suggested that this might result in a factor of 2 lower growth rate on forsteritic olivine compared to olivine in equilibrium with the melt. The mean crystal axes increase by a factor of 1.020 in going from forsterite to fayalite (Deer et al., 1992). If we assume that the expansion is linearly related to FeO/(FeO + MgO) and that the ratio in the initial olivine crystallizing from a typical type II chondrule was 0.25, we find that the initial mismatch in the size of the olivine axis between this olivine and a forsteritic relict grain would have been ~0.5%. Presumably, the way that the growing olivine deals with small mismatches is to grow patches of strained olivine interspersed by vacancies. Although the compositional gradient near the centers of large phenocrysts is small, near the surfaces of these grains igneous fractionation produced gradients as large as those in the overgrowths on low-FeO relicts. This suggests that the latter two growth rates may have been roughly comparable.

Another factor that would have ameliorated the mismatch is partial dissolution of the low-FeO relict that resulted in a FeO/(FeO + MgO) ratio in the adjacent boundary liquid that was intermediate between that in the relict and that in the bulk of the melt.

We therefore suggest that the mismatches between the growing olivine and the substrate may have been relatively small, and that Lofgren's estimate of a factor of 2 difference in growth rate is too high.

4.4. Almost Every CO Type-II Chondrule Contains Low-FeO Relict Grains

Steele (1989) found several low-FeO relicts in CO chondrules and noted that these are commonly mantled by ferroan olivine rims that are similar in composition to the outer margins of large olivine phenocrysts in the chondrules. Jones (1992) later investigated four type II chondrules in ALHA77307 and discovered that three included low-FeO relicts with ferroan olivine overgrowths.

As summarized in Table 2, we find that low-FeO relict grains are common to ubiquitous in type II chondrules from CO3.0 chondrites. Our detailed observations show that 10 of 11 investigated type II chondrules have such relicts; our SEM survey shows that 26 of 28 additional type II chondrules contain relict grains. Combining our statistics with those of Jones (1992) shows that 39 of 43 (91%) CO type II chondrules have low-FeO olivine relicts. The typical size of the investigated chondrules is 10–20× larger than the thickness of the thin section; thus, many relicts must have been missed. These observations imply that essentially all (>90%) large (≥300 μm) type II chondrules in these CO3.0 chondrites contain relicts.

This conclusion has important implications regarding the intensity of heating events in the nebular region where the type II CO chondrules were forming. There are two essential features that must have occurred during the formation of these chondrules: (a) they must have been preceded by the formation of low-FeO chondrules containing relatively coarse (≥10 μm) olivine grains (Jones and Scott, 1989; Jones, 1992); and (b) during the final melting event (and any other previous melting events in these chondrules), the amount of heat and the duration of heating were insufficient to destroy low-FeO precursor grains.

There are strong arguments for holding that most low-FeO

chondrules formed before most high-FeO chondrules. One of the most recent studies to show evidence of this was that of chondrules separated from the Lewis Cliff 85332 ungrouped carbonaceous chondrite. Wasson et al. (2000) found that low-FeO chondrules had unfractionated siderophile patterns, whereas the high-FeO patterns were fractionated, presumably because their precursors had undergone more stages of recycling. There is also O-isotopic evidence supporting this sequence; Jones et al. (2000) and Wasson (2000) noted that the $\Delta^{17}O$ of the chondrules correlated with chondrule type, with more positive values (those nearer the terrestrial composition) present in the type II chondrules. If, as various researchers (e.g., Rubin et al., 1990; Wasson, 2000) have inferred, nebular alteration causes the $\Delta^{17}O$ of fine-grained chondrule-precursor dust to move to higher values, the higher $\Delta^{17}O$ values of type II chondrules suggest that the precursors of these objects formed after those of type I chondrules. Thus, the common observation of low-FeO relicts is consistent with other evidence indicating that most low-FeO chondrules formed earlier than most high-FeO chondrules.

Greenwood and Hess (1996) used congruent melting models and experimental measurements to conclude that forsterite cannot have been at temperatures >2170 K in a molten chondrule for more than a few seconds without being resorbed into the melt. Clearly, the higher the FeO/(FeO + MgO) ratio, the lower the critical temperature. Although this temperature is much higher than would be calculated for incomplete (say, 50%) melting of these chondrules, any flash-heating mechanism that relies on the conduction of heat into grain centers requires a temperature spike that is higher than that present at the moment when the melt formed to achieve the high thermal gradients required to transport the heat into grains quickly.

4.5. Are High-FeO Relict Grains Also Ubiquitous?

We concluded above that low-FeO relict grains are ubiquitous in CO type II chondrules. We also showed that the central portions of the largest olivine grains in chondrule YcI were not melted in the final melting event (and, in this sense, are also relicts). This raises the question of whether a large fraction of the high-FeO phenocrysts in other type II chondrules are also relicts. We suspect that they are, and suggest some ways to test this conjecture.

The ideal information is the presence of asymmetric compositional profiles. Unfortunately, the interiors of large phenocrysts show only minor zoning, and a modest overgrowth is sufficient to obscure small asymmetries. A better alternative approach might be to demonstrate the presence of discontinuities in slope resulting when fragment compositions are very different from those of the overgrowths. This may be demonstrable in detailed EMP point profiles but geometric problems can obscure these effects. These hypothetical kinks in the FeO/(FeO + MgO) ratio should show up as linear or gently curved boundaries in carefully controlled BSE images or X-ray maps.

Above, we mentioned evidence that most low-FeO chondrules formed before most high-FeO chondrules. Nonetheless, there was a wide range of precursors available when the final generation of chondrules formed, and there were surely cases where large precursor grains had fayalite contents higher than the first solids to crystallize from the chondrule melt. In our view, the high-FeO core of an olivine grain in chondrule 41 of LL3.0 Semarkona (Fig. 4a,b of Jones, 1990) did not form in the final cooling event as Jones proposed. We believe that it is a high-FeO relict derived from a disrupted type II chondrule and mixed with the less-ferroan precursors of chondrule 41 before the final melting event. It is possible that this chondrule is an exception; if so, the apparent rarity of high-FeO relicts lends support to the idea that the mean FeO contents of chondrules gradually increased as the nebula evolved.

4.6. Formation of Large FeO-rich Chondrule Grains, Multiple Melting Events, and Sequential Formation of Low-FeO and High-FeO Chondrules in the CO Formation Region

Rubin (1989) noted that a significant fraction of type II porphyritic olivine chondrules in CO chondrites contain very coarse olivine phenocrysts that constitute 40–90 vol.% of the chondrule. He inferred that these are relict grains because dynamic crystallization experiments (Lofgren and Russell, 1986) had not produced such coarse crystals. In a later paper, Lofgren (1996) stated that coarse porphyritic chondrules have few, irregularly distributed nuclei derived from "precursor material with a much more heterogeneous grain size that may include some quite large crystals, on the order of 100's of microns." These experiments support our inference that the precursors of type II chondrules included coarse relict grains.

Our detailed studies of type II chondrules indicate that the final melting events were minor even though the whole chondrules have moderately low melting temperatures (because of their high FeO contents). Thus, the grains in these chondrules formed in several melting events. The question is then how many times did such chondrules melt while maintaining their basic porphyritic texture (i.e., without undergoing fragmentation or becoming enmeshed in and diluted to a major extent by foreign particles). To answer this question we will have to carry out much more detailed studies. We will need to gather enough compositional data to assess whether all phenocrysts appear to have formed from the same initial melt. The determination of minor elements using EMP analyses may be sufficient, but ion-probe studies of trace elements or O-isotopes may also be needed.

If the coarse crystals in chondrules such as YcA and YcI formed in a previous generation of chondrules, what were the processes that produced them? The only other type of FeO-rich chondrule that has reasonably coarse crystals are some of those with barred olivine (BO) textures. These objects formed by complete (or nearly complete) melting of the precursor assemblage, major undercooling, then nucleation at a few (perhaps 1–3) sites on the periphery. BO chondrules are rare, perhaps because chondrules were rarely heated long enough to destroy all nuclei. Thus, although fragmentation of ferroan, coarsely barred BO chondrules could have provided large phenocrysts to the precursor mix of type II chondrules, one must ask whether they were common enough to play this role. Our observations of Y81020 indicate that the type II-PO-chondrule/high-FeO-BO-chondrule ratio is ~20. It seems possible that BO chondrules were more abundant in an earlier nebular epoch when there was more turbulence to power the chondrule heating

events. It also seems possible that only ~5% of FeO-rich-chondrule heating events were sufficiently intense to cause total or near-total melting and form BO chondrules, but that, after these BO objects were produced, there were enough to supply the nuclei of the large phenocrysts in the type II PO chondrules.

An alternative is that the coarse phenocrysts grew in porphyritic chondrules (including the final porphyritic object) during repeated thermal events that produced low (perhaps 5–20%) degrees of melting. Along with these repeated minor melting events, there may have been hundreds of events that caused elevated temperatures but only incipient melting (Wasson, 1996).

5. SUMMARY

A high inferred cooling rate in a type II porphyritic olivine chondrule in the CO3.0 chondrite Yamato 81020 raised the question of how this observation could be reconciled with the large sizes of the coarse phenocrysts (the largest is 480 × 620 μm) in the same chondrule. Detailed petrographic examination of the chondrule showed the presence of many (~100) small (ca. 10 μm) olivine grains that grew after the last melting event. The centers of these grains have Fa contents of ≥47 mol.%; they clearly did not nucleate at the same time as the Fa26 olivine near the center of the large phenocryst. Further examination of additional chondrules in Y-81020 and ALHA77307 showed that low-FeO relict grains are ubiquitous in type II chondrules in CO3.0 chondrites. Our results, combined with those of Jones (1992), imply that >90% of the high-FeO chondrules in section contain low-FeO relicts; allowance for the fact that the chondrules are 10–20× thicker than the thin section leads to the conclusion that low-FeO relicts are present in nearly every type II chondrule. Each of these relicts has a high-FeO overgrowth with thicknesses ranging from 2 to 12 μm. Because the sections are, on average, somewhat oblique to the prime growth axes of the mineral grains, we conclude that the mean overgrowth thickness is ~4 μm. We suggest that these overgrowths can be produced in chondrules cooling at rates orders of magnitude greater than the commonly quoted range (0.01–1 K s^{-1}) based on furnace experiments. These small overgrowth thicknesses and the moderately high abundances of grains having recognizable fragmental shapes imply that the melt fraction in the final melting event was low, perhaps around 10%.

Acknowledgments— We thank R. H. Jones and J. N. Grossman for detailed and helpful reviews, T. L. Humphrys and T. Kunihiro for help with the SEM studies, and M. Yoshitake, K. Jo, J. Yim, and S. Zhang for technical assistance. This study was supported in part by NASA grant NAG 5-10421.

Associate editor: C. Koeberl

REFERENCES

Connolly H. C., and Hewins R. H. (1996) Constraints on chondrule precursors from experimental data. In *Chondrules and the Protoplanetary Disk* (eds. R. H. Hewins, R. H. Jones, and E. R. D. Scott), pp. 129-135. Cambridge University Press.

Deer W. A., Howie R. A., and Zussman J. (1992) *The Rock-Forming Minerals*, 2nd ed. Longman. 696 pp.

Donaldson C. H. (1976) An experimental investigation of olivine morphology. *Contrib. Mineral. Petrol.* **57,** 187–213.

Greenwood J. P., and Hess P. C. (1996) Congruent melting kinetics: Constraints on chondrule formation. In *Chondrules and the Protoplanetary Disk* (eds. R. H. Hewins, R. H. Jones, and E. R. D. Scott), pp. 205-211. Cambridge University Press.

Hewins R. H. (1988) Experimental studies of chondrules. In *Meteorites and the Early Solar System* (eds. J. F. Kerridge and M. S. Matthews), pp. 660-679. University of Arizona Press, Tucson.

Hood L. L. and Kring D. A. (1996) Models for multiple heating mechanisms. In *Chondrules and the Protoplanetary Disk* (eds. R. H. Hewins, R. H. Jones, and E. R. D. Scott), pp. 265-276. Cambridge University Press.

Jones R. H. (1990) Petrology and mineralogy of type II, FeO-rich chondrules in Semarkona (LL3.0): Origin by closed-system fractional crystallization, with evidence for supercooling. *Geochim. Cosmochim. Acta* **54,** 1785–1802.

Jones R. H. (1992) On the relationship between isolated and chondrule olivine grains in the carbonaceous chondrite ALHA77307. *Geochim. Cosmochim. Acta* **56,** 467–482.

Jones R. H. (1996) Relict grains in chondrules: Evidence for chondrule recycling. In *Chondrules and the Protoplanetary Disk* (eds. R. H. Hewins, R. H. Jones, and E. R. D. Scott), pp. 163-172. Cambridge University Press.

Jones R. H. and Lofgren G. E. (1993) A comparison of FeO-rich, porphyritic olivine chondrules in unequilibrated chondrites and experimental analogues. *Meteoritics* **28,** 213–221.

Jones R. H., Scott E. R. D. (1989) Petrology and thermal history of type IA chondrules in the Semarkona. (LL3.0) chondrite. *Proceedings Lunar and Planetary Science Conference.* 19:523–536.

Jones R. H., Saxton J. M., Lyon I. C., and Turner G. (2000) Oxygen isotopes in chondrule olivine and isolated olivine grains from the CO3 chondrite, ALHA77307. *Meteorit. Planet. Sci.* **35,** 849–857.

Lofgren G. E. (1989) Dynamic crystallization of chondrule melts of porphyritic olivine composition: Textures experimental and natural. *Geochim. Cosmochim. Acta* **53,** 461–470.

Lofgren G. E. (1996) A dynamic crystallization model for chondrule melts. In *Chondrules and the Protoplanetary Disk* (eds. R. H. Hewins, R. H. Jones, and E. R. D. Scott), pp. 187–196. Cambridge University Press.

Lofgren M. and Russell W. J. (1986) Dynamic crystallization of chondrule melts of porphyritic and radial pyroxene composition. *Geochim. Cosmochim. Acta* **50,** 1715–1726.

McSween H. Y. (1977) Chemical and petrographic constraints on the origin of chondrules and inclusions in carbonaceous chondrites. *Geochim. Cosmochim. Acta* **41,** 1843–1860.

Radomsky P. M. and Hewins R. H. (1990) Formation conditions of pyroxene-olivine and magnesian olivine chondrules. *Geochim. Cosmochim. Acta* **54,** 3537–3558.

Rubin A. E. (1989) Size-frequency distributions of chondrules in CO3 chondrites. *Meteoritics* **24,** 179–189.

Rubin A. E. and Krot A. N. (1996) Multiple heating of chondrules. In *Chondrules and the Protoplanetary Disk* (eds. R. H. Hewins, R. H. Jones, and E. R. D. Scott), pp. 173-180. Cambridge University Press.

Rubin A. E., Wasson J. T., Clayton R. N., and Mayeda T. K. (1990) Oxygen isotopes in chondrules and coarse-grained chondrule rims from the Allende meteorite. *Earth Planet. Sci. Lett.* **96,** 247–255.

Scott E. R. D. and Taylor G. J. (1983) Chondrules and other components in C, O, and E chondrites: Similarities in their properties and origins. *Proc. Lunar Planet. Sci. Conf.* **14,** B275–B286.

Steele I. M. (1989) Compositions and textures of relic forsterite in carbonaceous and unequilibrated ordinary chondrites. *Geochim. Cosmochim. Acta* **53,** 2069–2079.

Tsuchiyama A., Nagahara H., and Kushiro I. (1980) Experimental reproduction of textures of chondrules. *Earth Planet. Sci. Lett.* **48,** 155–165.

Wasson J. T. (1996) Chondrule formation: Energetics and length scales. In *Chondrules and the Protoplanetary Nebula* (eds. R. H. Hewins, R. Jones, and E. R. D. Scott), pp. 45-51. Cambridge University Press.

Wasson J. T. (2000) Oxygen-isotopic evolution of the solar nebula. *Rev. Geophys.* **38,** 491–512.

Wasson J. T., Kallemeyn G. W., and Rubin A. E. (2000) Chondrules in the LEW85332 ungrouped carbonaceous chondrite: Fractionation processes in the solar nebula. *Geochim. Cosmochim. Acta* **64,** 1279–1290.

Yurimoto H. and Wasson J. T. (2002) Extremely rapid cooling of a carbonaceous-chondrite chondrule containing very ^{16}O-rich olivine and a ^{26}Mg excess. *Geochim. Cosmochim. Acta* **66,** 4355–4363.